NEUROSCIENCE
RESEARCH ARTICLE

Mario J. Lintz et al. / Neuroscience 408 (2019) 191–203

Spatial representations in the superior colliculus are modulated by competition among targets

Mario J. Lintz,[abc] Jaclyn Essig,[ab] Joel Zylberberg[ab1] and Gidon Felsen[abc*]

[a]*Department of Physiology and Biophysics, University of Colorado School of Medicine, Aurora, CO 80045, United States of America*

[b]*Neuroscience Program, University of Colorado School of Medicine, Aurora, CO 80045, United States of America*

[c]*Medical Scientist Training Program, University of Colorado School of Medicine, Aurora, CO 80045, United States of America*

Abstract—Selecting and moving to spatial targets are critical components of goal-directed behavior, yet their neural bases are not well understood. The superior colliculus (SC) is thought to contain a topographic map of contralateral space in which the activity of specific neuronal populations corresponds to particular spatial locations. However, these spatial representations are modulated by several decision-related variables, suggesting that they reflect information beyond simply the location of an upcoming movement. Here, we examine the extent to which these representations arise from competitive spatial choice. We recorded SC activity in male mice performing a behavioral task requiring orienting movements to targets for a water reward in two contexts. In "competitive" trials, either the left or right target could be rewarded, depending on which stimulus was presented at the central port. In "noncompetitive" trials, the same target (e.g., left) was rewarded throughout an entire block. While both trial types required orienting movements to the same spatial targets, only in competitive trials do targets compete for selection. We found that in competitive trials, pre-movement SC activity predicted movement to contralateral targets, as expected. However, in noncompetitive trials, some neurons lost their spatial selectivity and in others activity predicted movement to ipsilateral targets. Consistent with these findings, unilateral optogenetic inactivation of pre-movement SC activity ipsiversively biased competitive, but not noncompetitive, trials. Incorporating these results into an attractor model of SC activity points to distinct pathways for orienting movements under competitive and noncompetitive conditions, with the SC specifically required for selecting among multiple potential targets.

Key words: Superior colliculus, decision making, target selection, freely-moving mice.

INTRODUCTION

Animals must select spatial targets and move to them to thrive in their natural environment. How the nervous system makes and how it acts on these spatial choices are fundamental questions in neuroscience. The superior colliculus (SC), a bilateral midbrain structure, is a critical node in an interconnected network of cortical and subcortical brain regions that have been shown to be involved in spatial orienting (Sparks, 1986; Krauzlis et al., 2004; Hikosaka et al., 2006; Gandhi and Katnani, 2011; Mysore and Knudsen, 2011; Wolf et al., 2015; Basso and May, 2017). Activity in the intermediate and deep layers of the SC is thought to represent targets, for movement and attention, in contralateral space (Wurtz and Goldberg, 1971; Robinson, 1972; Straschill and Rieger, 1973; McHaffie and Stein, 1982; Lee et al., 1988; Munoz et al., 1991; Glimcher and Sparks, 1992; Grantyn et al., 1996; Horwitz and Newsome, 1999; Felsen and Mainen, 2008; Krauzlis et al., 2013; Wang et al., 2015). These representations of spatial targets – which we refer to as "spatial representations" – are modulated by several factors, including the likelihood that the represented target will be selected, the value of the target, and the accuracy of the choice (Basso and Wurtz, 1997, 1998; Dorris and Munoz, 1998; Horwitz and Newsome, 2001; McPeek and Keller, 2002; Ikeda and Hikosaka, 2003; Felsen and Mainen, 2012; Odegaard et al., 2018), suggesting that the representations may be shaped by interactions among populations representing potential targets (Kim and Basso, 2008; Isa and Hall, 2009; Marino et al., 2011; Kardamakis et al., 2015). The observed modulation of SC spatial representations points to a potential role for the SC in mediating competition between targets underlying spatial choice. However, the effect of competition on spatial representations in the SC has not been directly examined.

*Corresponding author at: Department of Physiology and Biophysics, University of Colorado School of Medicine, 12800 E. 19th Ave., Mail Stop 8307, Aurora, CO 80045, USA. Tel.: +1 303 724 4532; fax: +1 303 724 4501.
E-mail address: gidon.felsen@ucdenver.edu (Gidon Felsen).

Abbreviations: SC, superior colliculus; E, excitatory; I, inhibitory; SNr, substantia nigra pars reticulata.

https://doi.org/10.1016/j.neuroscience.2019.04.002
0306-4522/

Specifically, to what extent are spatial representations modulated by competition among targets? Given the importance of these representations for orienting movements, demonstrating such modulation would suggest that the SC functions differently when a spatial choice is made (i.e., under "competitive" conditions) than when movements are made to a single target in the absence of alternatives (i.e., under "noncompetitive" conditions). We therefore examined spatial representations in the SC under these two conditions.

We reasoned that if SC representations depend on competition, we would observe a different relationship between SC activity and spatial targets when the targets do, and do not, compete for selection. We tested this idea by recording from the SC of mice performing a task in which identical spatial targets are selected under competitive and noncompetitive conditions (Lintz and Felsen, 2016). In the former condition, moving to the target at the left or right was a priori equally likely to be rewarded and therefore the targets competed to be selected, while in the latter, moving to only one of the targets would be rewarded, precluding any competition between the targets. We found that under competitive conditions, SC activity was higher preceding contraversive, rather than ipsiversive, movements (i.e., activity represented contralateral targets), consistent with previous studies (Horwitz and Newsome, 2001; Carello and Krauzlis, 2004; Kim and Basso, 2008; Thevarajah et al., 2009; Felsen and Mainen, 2012). However, under noncompetitive conditions, SC activity was nearly as likely to be higher preceding ipsiversive as contraversive movements. We then tested the causal relationship between the competition-dependence of SC activity and orienting movements by unilaterally silencing SC activity immediately preceding movement, and found that movements made under competitive conditions were biased ipsiversively, while those made under noncompetitive conditions were not directionally biased. Our results, along with simulated activity generated by a biologically-plausible attractor model, inform the distinct neural bases of orienting movements under competitive and noncompetitive conditions, and suggest that the SC plays a specific role in spatial choice.

EXPERIMENTAL PROCEDURES

Animal subjects

All experiments were performed according to protocols approved by the University of Colorado School of Medicine Institutional Animal Care and Use Committee. We used 10 male adult C57BL/6J mice (three for electrophysiology and seven for optogenetics experiments; aged 7–14 months at the start of experiments; Jackson Labs), housed in a vivarium with a 12-h light/dark cycle with lights on at 5:00 am. Food (Teklad Global Rodent Diet No. 2918; Harlan) was available *ad libitum*. Access to water was restricted to the behavioral session to motivate performance; however, if mice did not obtain 1 ml of water during the behavioral session, additional water was provided for ~2–5 min following the behavioral session (Thompson and Felsen, 2013; Lintz and Felsen, 2016). All mice were weighed daily and received sufficient water during behavioral sessions to maintain >85% of pre-water restriction weight.

Behavioral task

As described in Lintz and Felsen (2016), mice were first trained to perform "competitive" trials and were then trained to perform "noncompetitive" trials [we previously referred to these trial types as "stimulus-guided" and "internally-specified," respectively (Lintz and Felsen, 2016)]. Training on competitive trials was identical to training on the odor-guided spatial choice task (Uchida and Mainen, 2003) described in Stubblefield et al. (2013). Briefly, each mouse was water-restricted and trained to interact with three ports (center: odor port; sides: reward ports) along one wall of a behavioral chamber (Island Motion). In each trial, the mouse entered the odor port, triggering the delivery of an odor; waited 300–500 ms for a go signal (auditory tone); exited the odor port; and entered one of the reward ports (Fig. 1*A*). Premature exit from the odor port resulted in the unavailability of reward in that trial. Varying the duration of the delay preceding the go signal prevents the mouse from predicting precisely when movement can be initiated, allowing us to disambiguate neural activity related to movement initiation from that that related to other functions (e.g., target selection or motor planning). Odors were comprised of binary mixtures of (+)-carvone and (−)-carvone, commonly perceived as caraway and spearmint, respectively; an enantiomeric odor pair was selected to control for differences in molecular structure of odorant stimuli. In each competitive trial, one of seven odor mixtures was presented via an olfactometer (Island Motion): volume (+)-carvone/(−)-carvone = 95/5, 80/20, 60/40, 50/50, 40/60, 20/80, or 5/95. Mixtures in which (+)-carvone > (−)-carvone indicated reward availability only at the right port and mixtures in which (−)-carvone > (+)-carvone indicated reward availability only at the left port [we therefore refer to (−)-carvone as the "left odor" for simplicity]. In trials in which (+)-carvone = (−)-carvone, the probability of reward at the left and right ports, independently, was 0.5. Reward, consisting of 3 μl of water, was delivered by transiently opening a calibrated water valve 10–100 ms after reward port entry. Odor and water delivery was controlled, and port entries and exits were recorded, using custom MATLAB (MathWorks) software (adapted from C. D. Brody).

Mice learned to perform competitive trials within ~39 sessions (1 session/day); detailed training stages are described in Stubblefield et al. (2013). Mice required an additional ~5 sessions to learn to perform interleaved blocks of competitive and noncompetitive trials. In every noncompetitive trial the 50/50 mixture of (+)-carvone/(−)-carvone was presented, and reward was available only at one side throughout the block. Mice were first introduced to interleaved blocks, each of which required 25 correct trials to advance to the next block. Once they performed ~70% of trials in the session correctly, the number of correct trials required per block was increased to 50. Mice performed 5 blocks per session, starting with a competitive block and alternating between competitive and noncompetitive blocks (Fig. 1*B*); the side associated with reward switched between each noncompetitive block. Upon

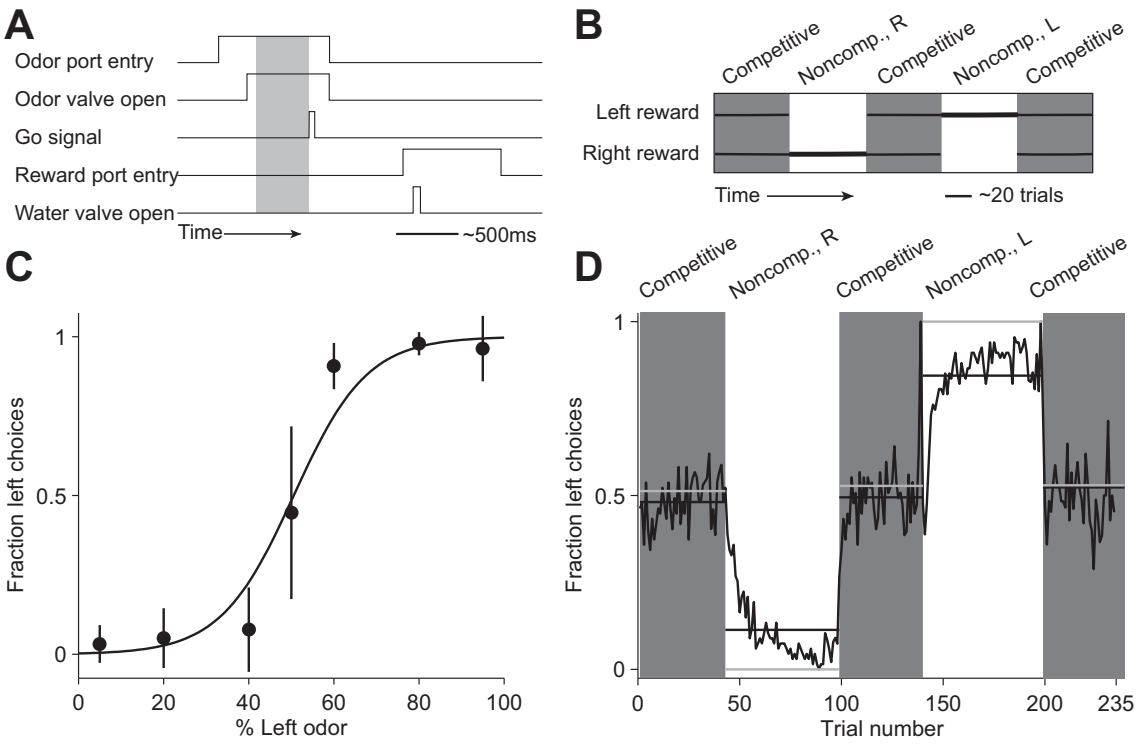

Fig. 1. Performance on behavioral task requiring movements to targets under competitive and noncompetitive conditions.*A*: Timing of trial events. In all trials, the mouse enters the central odor port, is presented with an odor mixture, waits for the go signal, exits the odor port, moves to one of the side reward ports, and receives water for a correct choice. The gray box shows the delay epoch in which neuronal activity is analyzed and manipulated, below.*B*: Organization of competitive (gray) and noncompetitive (Noncomp., white) blocks within a session. In competitive blocks, reward side corresponds to the dominant odor in the mixture [(−)-carvone, left; (+)-carvone, right]; when the odors are balanced ([(−)-carvone] = [(+)-carvone]), the probability of reward at both reward ports is 0.5. In noncompetitive blocks, odors are balanced in every trial and reward is available at the same side [left (L) or right (R)] in each trial. Thickness of horizontal lines corresponds to probability of reward in the block.*C*: Mean performance in competitive trials across all sessions (three mice). Line shows best fit to $p = \frac{1}{1+e^{-a-bx}}$, where *x* is the proportion of the left odor [(−)-carvone)] in the mixture, *p* is the average fraction of leftward choices, and *a* and *b* are free parameters. Choices were strongly dependent on the dominant component of the odor mixture. Error bars, ± SD across sessions.*D*: Mean fraction of left choices over all sessions (three mice). Horizontal black lines show block means; gray lines show ideal block means (if all choices were correct). Since different numbers of trials per block were performed across sessions, trials that occur in <60% of sessions are excluded. In competitive blocks only difficult trials [(+)-carvone/(−)-carvone = 60/40, 50/50, or 40/60] are shown.

completing training, mice were implanted with microdrives for neuronal recording or optical fibers for light delivery (see below).

Surgery

Details of the surgical procedure are provided in Thompson and Felsen (2013). Briefly, once the mouse was fully trained on the task, it was anesthetized with isoflurane and secured in a stereotaxic device, the scalp was incised and retracted, two small screws were attached to the skull, and a craniotomy targeting the left SC was performed, centered at 3.88 mm posterior from bregma and 1.0 mm lateral from the midline (Paxinos and Franklin, 2004). A VersaDrive 4 microdrive (Neuralynx), containing four independently adjustable tetrodes, was affixed to the skull via the screws, luting (3M), and dental acrylic (A-M Systems). A second small craniotomy was performed to place the ground wire in direct contact with the brain. After the acrylic hardened, a topical triple antibiotic ointment (Major) mixed with 2% lidocaine hydrochloride jelly (Akorn) was applied to the scalp, the mouse was removed from the stereotaxic device, the isoflurane was turned off, and oxygen alone was delivered to the animal to gradually alleviate anesthetic state. Mice were administered sterile isotonic saline (0.9%) for rehydration and an analgesic (Ketofen; 5 mg/kg) for pain management. Analgesic and topical antibiotic administration was repeated daily for up to 5 days, and animals were closely monitored for any signs of distress.

This surgical procedure was adapted for injecting viral vectors and implanting optical fibers to the same location in the left SC as above (using the same rostrocaudal and mediolateral coordinates, and targeting the fiber tip to the dorsal surface of the intermediate layer). Based on a similar strategy for inhibiting excitatory SC neurons (Kopec et al., 2015), we obtained expression of eArch 3.0 in these neurons by injecting adult mice with 600 nl of pAAV-CaMKIIα-eArch3.0-EYFP [obtained from the University of North Carolina Vector Core with permission from Dr. Karl Deisseroth (Stanford University)]. An optical fiber was permanently implanted as part of a moveable drive housing (Anikeeva et al., 2011) to deliver light to opsin-expressing neurons located ventral to the fiber tip. Optogenetic experiments were performed at least 3 weeks following virus injection.

Electrophysiology

Neuronal recordings were collected using four tetrodes, wherein each tetrode consisted of four polyimide-coated nichrome wires (Sandvik; single-wire diameter 12.5 μm) gold plated to 0.2–0.4 MΩ impedance. We have found that this impedance is the lowest we can reliably achieve using standard gold-plating methods, and that it is well-suited for obtaining signals from which we can reliably isolate the activity of individual neurons in the mouse brain (Lintz and Felsen, 2016; Stubblefield et al., 2015; Thompson and Felsen, 2013; Thompson et al., 2016). Electrical signals were amplified and recorded using the Digital Lynx S multichannel acquisition system (Neuralynx) in conjunction with Cheetah data acquisition software (Neuralynx).

Tetrode depths were adjusted approximately 23 h before each recording session to sample an independent population of neurons across sessions. To estimate tetrode depths during each session we calculated distance traveled with respect to rotation fraction of the screw that was affixed to the shuttle holding the tetrode. One full rotation moved the tetrode ~250 μm and tetrodes were moved ~62.5 μm between sessions. The final tetrode location was confirmed through histological assessment using electrolytic lesions and tetrode tracks (see below).

Offline spike sorting and cluster quality analysis was performed using MClust software (MClust-3.5, A.D. Redish) in MATLAB. Briefly, for each tetrode, single units were isolated by manual cluster identification based on spike features derived from sampled waveforms. Identification of single units through examination of spikes in high-dimensional feature space allowed us to refine the delimitation of identified clusters by examining all possible two-dimensional combinations of selected spike features. We used standard spike features for single unit extraction: peak amplitude, energy (square root of the sum of squares of each point in the waveform, divided by the number of samples in the waveform), and the first principal component normalized by energy. Spike features were derived separately for individual leads. To assess the quality of identified clusters we calculated two standard quantitative metrics: L-ratio and isolation distance (Schmitzer-Torbert et al., 2005). Clusters with an L-ratio of less than 0.82 and isolation distance greater than 3 were deemed single units. We did not observe any relationship between clustering metrics and the functionally-identified neuron types described in the Results. Units were clustered blind to interspike interval, and only clusters with few interspike intervals <1 ms were considered for further examination. Furthermore, we excluded the possibility of double counting neurons by ensuring that both the waveforms and response properties sufficiently changed across sessions. If they did not, we conservatively assumed that we recorded twice from the same neuron, and only included data from one session.

Optogenetic stimulation

Light was delivered via a diode-pumped, solid-state laser (532 nm; Shanghai Laser & Optics Century) coupled to a 105 μm-diameter optic fiber (numerical aperture: 0.22), calibrated daily with an optic power meter (Melles Griot) to deliver 20–24 mW to the intermediate and deep layers of the left SC (Al-Juboori et al., 2013). Within each of seven mice used in these experiments, the same site was stimulated across sessions. Light was delivered continuously for 300–400 ms of the delay epoch (from 100 ms after odor valve open until the go signal) on ~25% of trials; we observed no differences between several protocols with slightly different timing and therefore combined the resulting data.

Lesioning and Histology

To verify final tetrode location we performed electrolytic lesions (100 μA, ~1.5 min per lead) after the last recording session. One day following lesion, mice were overdosed with an intraperitoneal injection of sodium pentobarbital (100 mg/kg) and transcardially perfused with saline followed by ice-cold 4% paraformaldehyde (PFA) in 0.1 M phosphate buffer (PB). After perfusion, brains were submerged in 4% PFA in 0.1 M PB for 24 h for post-fixation and then cryoprotected for 24 h by immersion in 30% sucrose in 0.1 M PB. The brain was encased in the same sucrose solution, and frozen rapidly on dry ice. Serial coronal sections (60 μm) were cut on a sliding microtome for reconstruction of the lesion site and tetrode tracks. Fluorescent Nissl (NeuroTrace, Invitrogen) was used to identify cytoarchitectural features of the SC and verify tetrode tracks and lesion damage within or below the SC. Images of the SC were captured with a 10× objective lens, using a 3I Marianis inverted spinning disc confocal microscope (Zeiss). Arch expression and optical fiber depth were verified followed the same procedures with the exception of electrolytic lesioning, and allowed us to confirm that effective optical stimulation was limited to the intermediate and deep layers of the left SC.

Attractor model

To examine how SC activity might differ between competitive and noncompetitive conditions, we constructed a "bump attractor" model (modified from Wimmer et al., 2014) consisting of 200 excitatory (*E*) neurons and 100 inhibitory (*I*) neurons per SC (600 neurons total), an *E*:*I* ratio consistent with the intermediate and deep layers of the mammalian SC (Mize, 1992; Sooksawate et al., 2011). Unlike the model of Wimmer et al. (2014), wherein neurons are positioned on a ring, neurons in our model are positioned along a line, to better match the structure of the SC. We defined neuron position with respect to the rostrocaudal axis: position 0 corresponds to the most rostral pole of the SC, and position 1 corresponds to the most caudal end. Intra-SC synaptic weights were larger for nearby neurons, and smaller for more distant ones, determined by.

$$W_{ij} = amp * e^{\frac{-(i-j)^2}{scale^2}}, \quad (1)$$

where *i* and *j* are the locations of the pre- and post-synaptic neurons along the rostrocaudal axis, respectively,

and *amp* and *scale* are defined independently for presynaptic *E* and *I* neurons (amp_E = 0.1, amp_I = 2, $scale_E$ = 0.055, $scale_{Irostral}$ = 0.78, $scale_{Icaudal}$ = 0.73; rostral: $i < 0.25$). *amp* sets the amplitude of the connection weights, and *scale* determines the spatial extent over which the connection strength decays. To promote network stability, each *W* was normalized to have a maximum eigenvalue of 1.5 by dividing all connection values by max(λ)/1.5, where max(λ) is the largest eigenvalue of the matrix after initialization.

Reciprocal inter-SC connections consisted of the 10 most rostral *I* neurons synapsing with weight 2/max(λ) onto *E* and *I* neurons at the corresponding location in the contralateral SC. Membrane potentials and corresponding spike rates of *E* and *I* neurons in the left SC (v_E^L, v_I^L, r_E^L and r_I^L, respectively) evolved at each time step (~2 ms in our numerical simulations) according to

$$\begin{aligned}\frac{dv_E^L}{dt} &= -v_E^L + W_{EE}^L r_E^L - W_{IE}^L r_I^L - W_{R\to L_{IE}}^L r_I^R + external^L \\ &+ noise \\ \frac{dv_I^L}{dt} &= -v_I^L - W_{II}^L r_I^L + W_{EI}^L r_E^L - W_{R\to L_{II}}^L r_I^R \\ &+ noise,\end{aligned} \tag{2}$$

and all spike rates were rectified at each time step according to.

$$r = \begin{cases} 0, & \text{for } v < 0 \\ v, & \text{for } 0 < v < 100 \\ 100, & \text{for } v > 100 \end{cases}, \tag{3}$$

where, e.g., W_{EE}^L represents synaptic weights from left *E* to *E* neurons, W_{IE}^L represents weights from left *I* to *E* neurons, and $W_{R\to L_{IE}}^L$ represents weights from right *I* to left *E* neurons. *Noise* was drawn from a Gaussian distribution with mean = 0, and variance = 25 for *E* neurons and 16 for *I* neurons. r_E^L and r_I^L are vectors, with one entry per *E* or *I* neuron in the left SC, respectively. Similarly, r_E^R and r_I^R describe the firing rates of neurons in the right SC, and they evolve over time via the same equations as those in the left SC (i.e., via Eqs. ((2) and ((3), with all "*L*"s replaced by "*R*"s).

The vectors $external^L$ and $external^R$ represent the drive to each neuron from sources outside the SC. For all trial types, external drive was applied to *E* neurons only, in a linearly graded fashion along the rostrocaudal axis. In competitive leftward trials, the right SC receives a stronger external drive than the left SC, and vice versa in competitive rightward trials. In noncompetitive trials, the left and right SC received equal drive; half of these trials were assigned to be leftward and half rightward. Specifically, in competitive leftward trials, the drive to left SC neuron *i* was $external_i^L = 3i + 0.7$, and the drive to right SC neuron *i* was $external_i^R = 5i + 0.7$; and in competitive rightward trials, the drive to left SC neuron *i* was $external_i^L = 5i + 0.7$, and the drive to right SC neuron *i* was $external_i^R = 3i + 0.7$. In noncompetitive trials, the drive to SC neuron *i* in both SCs was $external_i = 3i + 0.7$. For all trial types, external drive was applied for the first 150 time steps (~300 ms) of the simulation, representing the beginning of the trial, and was then set to 0.

Overall, this model structure generates a "bump" of activity around the location at which the external drive is strongest, sustained by the excitation of nearby neurons and the inhibition between distant neurons even once the external drive is removed. In general we found that the small changes from our final parameter values did not affect either the emergence of the bump or our overall results. We considered the first 200 time steps (~400 ms) of the simulation to describe our "delay epoch" (defined below for our neuronal recordings), and calculated the average firing rate of each neuron during this epoch in each trial. Each "session" consisted of 50 leftward and 50 rightward trials in each condition (competitive and noncompetitive). We ran our simulation for 20 such sessions and randomly selected ~3 caudal SC neurons from each session, to match the number and location of buildup neurons recorded in each experimental session. Finally, for each neuron we calculated direction preference based on the simulated firing rates in leftward and rightward trials as we did for the experimentally recorded neurons (see "Direction preference," below).

Experimental design and statistical analyses

Electrophysiological recordings were obtained from 172 SC neurons in 67 behavioral sessions from three mice. Optogenetic manipulation experiments were performed in 82 behavioral sessions from seven additional mice. Details of our analyses of the data obtained from our recording and manipulation experiments are described immediately below. For comparisons across conditions (e.g., firing rate during competitive vs. noncompetitive trials), we generally used paired two-tailed t-tests; χ^2-tests and ANOVAs were also used when appropriate. All analyses were performed in MATLAB.

Direction preference

To examine the dependence of the firing rate of individual neurons on movement direction, we used an ROC-based analysis (Green and Swets, 1966) that quantifies the ability of an ideal observer to classify whether a given spike rate during the delay epoch was recorded in one of two conditions (here, preceding leftward or rightward movement). We defined the delay epoch as beginning 100 ms after odor valve open [to account for the empirically-measured delay between odor valve open and odor detectability at the port (Thompson and Felsen, 2013)] and ending with the go signal. We defined "preference" as 2(ROCarea − 0.5), a measure ranging from −1 to 1, where −1 denotes the strongest possible preference for left, 1 denotes the strongest possible preference for right, and 0 denotes no preference (Feierstein et al., 2006). Statistical significance was determined with a permutation test: we recalculated the preference after randomly reassigning all firing rates to either of the two groups arbitrarily, repeated this procedure 500 times to obtain a distribution of values, and calculated the fraction of random values exceeding the actual value. We tested for significance at α = 0.01. Trials in which the movement time (between odor port exit and reward port entry) was >1.5 s were excluded from all analyses. Neurons with fewer than

100 competitive or noncompetitive trials, or with a firing rate below 2.5 spikes/s across the entire session for either competitive or noncompetitive trials, were excluded from all analyses.

Optogenetic effect on behavior

To compare the effect of optogenetic inhibition between competitive and noncompetitive trials, we calculated, separately for competitive and noncompetitive trials and for trials in which leftward and rightward movements were correct, the difference between the fraction of correctly performed trials in which light was and was not delivered. We then averaged these light-induced differences to calculate the "% bias," separately for competitive and noncompetitive trials, after inverting the sign for trials in which the leftward movement was correct, such that negative values of % bias correspond to a leftward (ipsiversive) shift and positive values to a rightward (contraversive) shift. For trials with 50/50 mixtures of (+)-carvone/(−)-carvone, either choice was considered correct.

RESULTS

Mice were trained on a delayed-response spatial orienting task. In each trial of the task, the mouse was presented with a binary odor mixture at a central port, waited for an auditory go cue, and moved to the left or right reward port for a water reward (Fig. 1*A*). Within each session, blocks of competitive and noncompetitive trials were interleaved. In competitive trials, the dominant component of the odor mixture – which varied trial by trial – determined the side at which reward would be delivered. In noncompetitive trials, a balanced mixture of the two odors was always presented but reward was delivered at only one side throughout the block (Fig. 1*B*). Thus, while both trial types required the mouse to sample the stimulus and initiate an orienting movement to a reward port, both reward ports (left and right) were viable options in a given competitive trial, whereas only one reward port (left or right) was a viable option in a given noncompetitive trial (Ito and Doya, 2015; Lintz and Felsen, 2016; Pastor-Bernier and Cisek, 2011; Siniscalchi et al., 2016; see Experimental Procedures). As we have previously shown (Lintz and Felsen, 2016), mice were able to infer (unsignaled) transitions between the competitive and noncompetitive blocks and switch their response mode accordingly. During competitive blocks, choices depended on the dominant component of the odor mixture (Fig. 1*C*), which was equally likely to signal reward at the left or right port, resulting in the left and right port being equally likely to be chosen (Fig. 1*D*, gray boxes). During noncompetitive blocks, mice reliably returned to the same (rewarded) port in each trial (Fig. 1*D*, white boxes). These data suggest that, as intended, the direction of movement in competitive blocks was selected based on the stimulus, which was equally likely to indicate reward at the left and the right, while in noncompetitive blocks the direction of movement was selected based on recent experience indicating reward at only one side. We therefore utilized this behavioral assay to compare SC activity under conditions in which spatial targets do and do not compete for selection.

We recorded from 172 well-isolated left SC neurons (see Experimental Procedures, Fig. 2) in three mice performing the behavioral task. We focused on neuronal activity during the delay epoch, defined as the period starting 100 ms after odor valve opening and ending at the time of the auditory go signal (Fig. 1*A*, gray box), which most directly captures activity underlying the selection, planning, and preparation of movement to the reward port (Thompson and Felsen, 2013). Based on activity during this epoch of competitive trials, we qualitatively classified 118 neurons into categories described in primate and cat SC that are thought to play distinct functional roles (Glimcher and Sparks, 1992; Munoz and Guitton, 1991; Munoz et al., 1991; Munoz and Wurtz, 1993, 1995; Hafed et al., 2009). One group of neurons (50/172; Fig. 3*A*) typically exhibited a gradual increase in firing rate leading up to, and a rapid increase during, movement initiation, similar to the "buildup" (or "prelude") neurons previously described (Glimcher and Sparks, 1992; Munoz and Wurtz, 1995; Munoz et al., 1991). A second group exhibited a rapid increase during movement initiation (49/172; Fig. 3*B*), akin to "burst" neurons (Munoz and Wurtz, 1995). A third group exhibited the opposite, a decrease in activity during movement initiation (19/172; Fig. 3*C*). These "pause" neurons bear some similarity to the "fixation" neurons described in primate and cat SC (Munoz and Guitton, 1991; Munoz and Wurtz, 1993), given that they are more active when still than when initiating movement, but they may play a distinct functional role. The remaining 54/172 neurons exhibited activity that did not clearly resemble these previously-described classes, which is not surprising since we did not select any particular type of neurons before beginning the behavioral session, and since there remains debate over whether these classes are entirely distinct (e.g., fixation neurons in primate may be considered burst neurons with small preferred movement amplitudes (Hafed and Krauzlis, 2012)). Although these classes were initially defined in the context of eye movements performed by head-fixed primates and cats, typically in response to visual stimuli, the fact that qualitatively similar activity is observed in freely-moving mice making full-body movements is consistent with a conserved role for the SC in orienting movements (Gandhi and Katnani, 2011; Wolf et al., 2015; Basso and May, 2017).

To examine spatial representations in the SC, we next calculated the direction preference during the delay epoch of all competitive trials in which a reward port was selected; preference ranges from −1 (strongly "prefers" ipsiversive) to 1 (strongly prefers contraversive), where 0 represents no preference (Experimental Procedures). Among buildup neurons, we found that 22/50 displayed a significant direction preference ($p < 0.01$, Monte Carlo permutation test), with nearly all preferring contraversive (21/22) rather than ipsiversive (1/22) choices (Fig. 3*D*; $p = 2.0 \times 10^{-5}$, χ^2-test). This fraction of direction-selective neurons – and the bias toward contraversive choices in buildup activity – is consistent with previous studies of spatial choice in the SC (Horwitz and Newsome, 2001; Hirokawa et al., 2011; Felsen

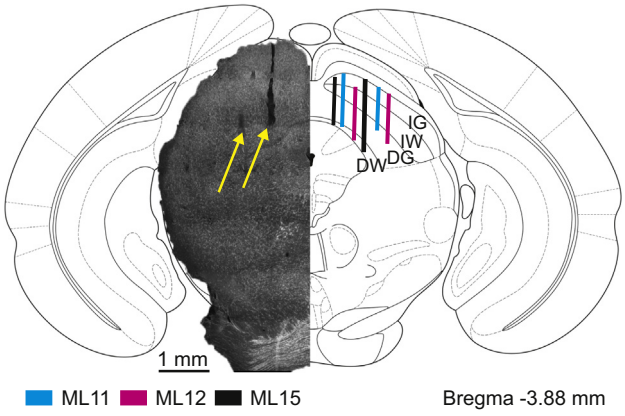

Fig. 2. Confirmation of tetrode recording sites.Coronal section (left, 3.88 mm caudal from bregma) shows representative tetrode tracks (arrows) in SC; schematic (right), from Paxinos and Franklin (2004), shows targeted recording extent (colored bars) within SC of two tetrodes for each recorded mouse in the study; the other two tetrodes for each mouse were at similar mediolateral and dorsoventral extents in a different coronal plane. Neurons recorded at locations outside of the intermediate and deep layers of the SC, determined histologically, were excluded from analysis. IG, intermediate gray layer; IW, intermediate white layer; DG, deep gray layer; DW, deep white layer.

and Mainen, 2012). We also found that, based on post-hoc histological estimates of recording sites (Fig. 2), direction preference was stronger at more lateral sites ($p = 1.3 \times 10^{-8}$, one-way ANOVA), suggesting that approach-related neurons in the lateral SC may drive spatial choice more than avoidance-related neurons in the medial SC (Dean et al., 1989). Among burst and pause neurons, only 4/49 (Fig. 3*E*) and 1/19 (Fig. 3*F*), respectively, displayed a significant ($p < 0.01$, Monte Carlo permutation test) direction preference during the delay epoch, although many of these neurons exhibited direction preference in other epochs (e.g., Fig. 3, *B* and *C*), consistent with previous findings (Felsen and Mainen, 2008).

We next examined whether SC activity differed between competitive and noncompetitive trials. We focused on buildup neurons over burst and pause neurons since a sizeable fraction of the former exhibited direction preference during the delay epoch, consistent with buildup neurons being most closely associated with spatial choice and other decision-related functions (Dorris et al., 1997; Horwitz and Newsome, 1999; McPeek and Keller, 2002; Kim and Basso, 2008; Felsen and Mainen, 2012). Fig. 4*A* shows data from another example neuron, separately for competitive and noncompetitive trials. During the delay epoch, there appears to be a difference in activity between these trial types, even when the same reward port is selected. To quantify this phenomenon across the population, we examined how direction preference calculated in noncompetitive trials compared to that calculated in competitive trials (as in Fig. 3*D*). In stark contrast to the strong bias toward contraversive preference during competitive trials [Fig. 4*B*, filled gray circles; 21/50 preferred contraversive, 1/50 preferred ipsiversive (same data as black bars in Fig. 3*D*)], in noncompetitive trials, neurons were as likely to show no direction preference, or even to prefer ipsiversive movement, as they were to exhibit a contraversive preference (Fig. 4*B*, filled black circles; 15/50 preferred contraversive and 15/50 preferred ipsiversive). In particular, nine neurons with a contraversive preference in competitive trials exhibited no preference in noncompetitive trials, three neurons with a contraversive preference in competitive trials exhibited an ipsiversive preference in noncompetitive trials, and 17 neurons with no preference in competitive trials exhibited a preference in noncompetitive trials (11 ipsiversive, six contraversive).

This fundamental difference in preference between trial types was driven mainly by higher activity in contraversive competitive as compared to noncompetitive trials (Fig. 4*C*; contraversive trials: $p = 0.022$; ipsiversive trials: $p = 0.34$, paired two-tailed t-tests; activity appears to decrease gradually over the course of contraversive noncompetitive blocks), and was not due to changes in overall firing rate over the course of the session (e.g., due to recording instability; $p = 0.70$, one-way ANOVA of firing rate across session quartiles; Fig. 4*D*), the fact that only the 50/50 odor mixture was presented in noncompetitive trials (activity did not depend on the difficulty of the discrimination: contraversive trials, $p = 0.31$; ipsiversive trial,: $p = 0.44$, paired two-tailed t-tests; preference computed for all competitive trials was highly correlated with preference computed for only 50/50 competitive trials: $r = 0.70$, $p = 1.33 \times 10^{-7}$), or to the mediolateral coordinate of the recording site. Notably, we observed this effect – lower activity in contraversive noncompetitive than competitive trials (Fig. 4*C*) – despite the higher probability of movement to the contralateral port in blocks of noncompetitive rightward than competitive trials, which has been shown to elicit higher SC activity (Basso and Wurtz, 1997, 1998). Neither could this effect be explained by differences in reaction time (duration between the go signal and odor port exit) between noncompetitive and competitive trials. While we often observed shorter reaction times in noncompetitive than competitive trials (29/66 sessions; $p < 0.05$, unpaired two-tailed t-test), which are consistent with previous results (Lintz and Felsen, 2016), in only 1 of the 22 build-up neurons with a significant direction preference in competitive trials (Fig. 3D, black bars) did firing rate decrease with shorter reaction times ($p < 0.05$, Pearson's r). Finally, we reasoned that, because the direction of movement can be anticipated even before the delay epoch in noncompetitive trials, neurons might simply exhibit the expected contraversive direction preference during an earlier epoch. We therefore calculated preference in noncompetitive trials during the epoch from odor port entry until 100 ms after odor valve open. As was the case in the delay epoch, we found that neurons were just as likely to prefer ipsiversive as contraversive movements (Fig. 4*E*; 16/50 preferred contraversive and 15/50 preferred ipsiversive). These data demonstrate that the neuronal representation of movements to contralateral space, a hallmark of SC function (Gandhi and Katnani, 2011), appears to be strikingly dependent on whether targets compete for selection.

To test the causal relationship between these spatial representations and movement direction, we examined the

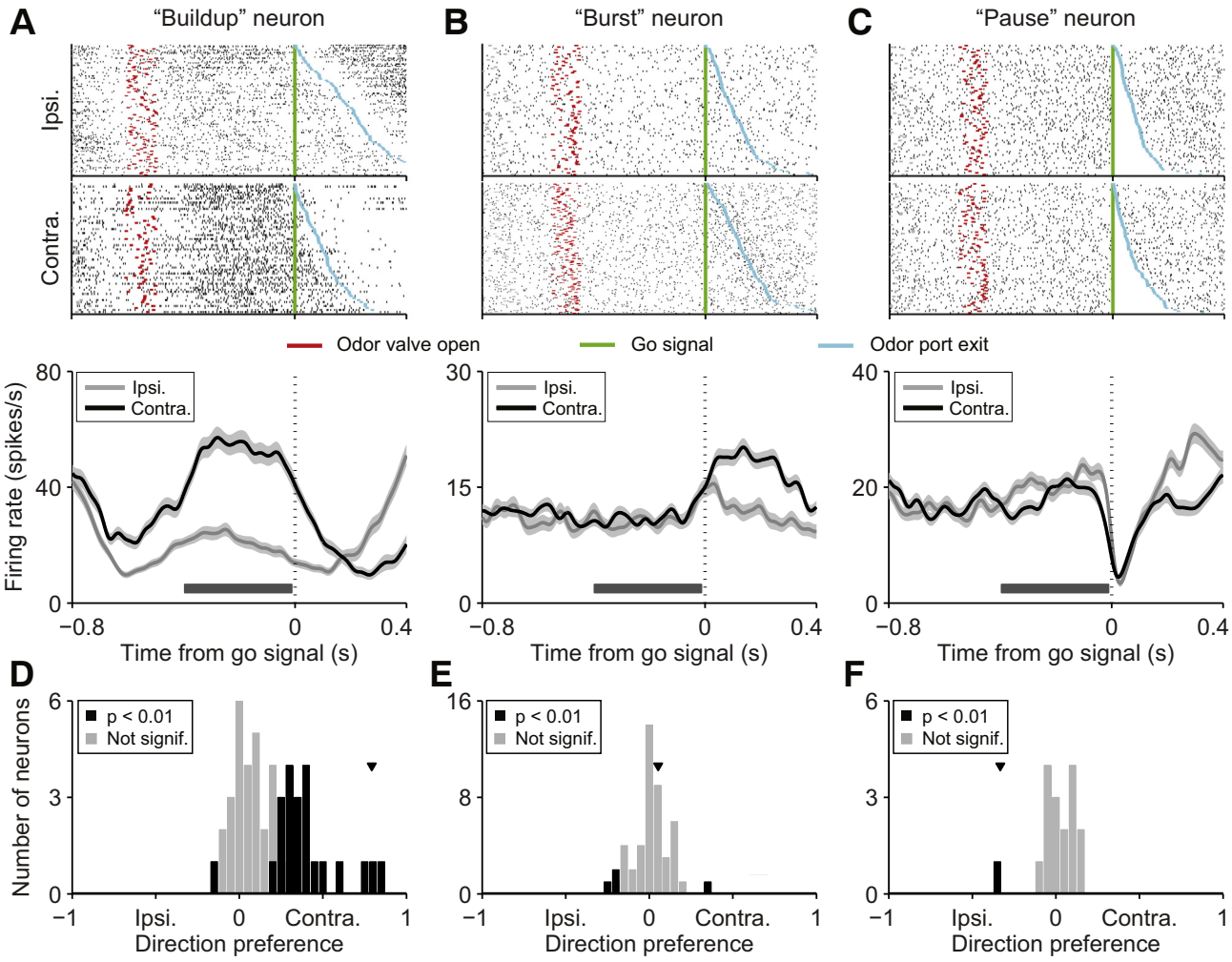

Fig. 3. Activity of functionally classified SC types in competitive trials.*A*: Rasters (upper) and peri-event histograms (lower) for an example buildup neuron grouped by movement direction. For each raster, each row shows spikes (black ticks) in one trial, aligned to time of go signal (green line) and sorted by relative time of odor port exit. Red ticks, times of odor valve open; blue ticks, times of odor port exit. Fifty pseudo-randomly selected trials are shown per group. Peri-event histograms show average activity separately for trials of each movement direction. Shading, ± SEM. Histograms are smoothed with a Gaussian filter (σ = 15 ms). Gray bar shows mean delay epoch. Ipsi., ipsiversive; Contra., contraversive.*B*: Same as *A*, for an example burst neuron.*C*: Same as *A*, for an example pause neuron.*D*: Direction preferences during delay epoch of competitive trials across population of buildup neurons. Bar segments corresponding to neurons with significant preference ($p < 0.01$) are shown in black. Arrowhead corresponds to example neuron in *A*.*E*: Same as *D*, for population of burst neurons.*F*: Same as *D*, for population of pause neurons. (For interpretation of the references to color in this figure legend, the reader is referred to the web version of this article.)

behavioral effect of unilaterally inhibiting SC activity during the delay epoch. Previous manipulation experiments have shown that, under competitive conditions, SC activity promotes contraversive choices (McPeek and Keller, 2004; Felsen and Mainen, 2008; Stubblefield et al., 2013; Duan et al., 2015; Kopec et al., 2015), consistent with the contraversive direction preference that we and others have observed (Fig. 3*D*; Horwitz and Newsome, 2001; Hirokawa et al., 2011; Felsen and Mainen, 2012). We reasoned that, since the contraversive bias in direction preference is absent in noncompetitive trials (Fig. 4*B*), unilaterally inhibiting a population of SC neurons during these trials would have little net effect on movement direction. We tested this prediction by optogenetically inhibiting activity in the intermediate and deep layers of the left SC during the delay epoch via light-mediated activation of Arch-expressing excitatory neurons (Fig. 5*A*; Experimental Procedures; 77 sessions). As expected, unilateral inhibition in competitive trials produced a small ipsiversive bias (Fig. 5, *B* and *C*; $p = 0.016$, paired two-tailed t-test comparing % bias to 0; Stubblefield et al., 2013; Kopec et al., 2015). However, the identical stimulation in noncompetitive trials resulted in a smaller directional bias that did not differ significantly from 0 (Fig. 5*C*; $p = 0.16$, paired two-tailed t-test comparing % bias to 0). We confirmed in control sessions that the presence of the fiber itself in the SC, and any light potentially visible from the fiber, did not affect behavior by repeating these experiments with light blocked at the coupling ferrule before entering the brain, and saw no effect of light delivery for either trial type (Fig. 5*C*; competitive: $p = 0.67$; noncompetitive: $p = 0.63$, paired two-tailed t-tests comparing % bias to 0; 5 sessions). Although the control data were somewhat more variable, owing in part to

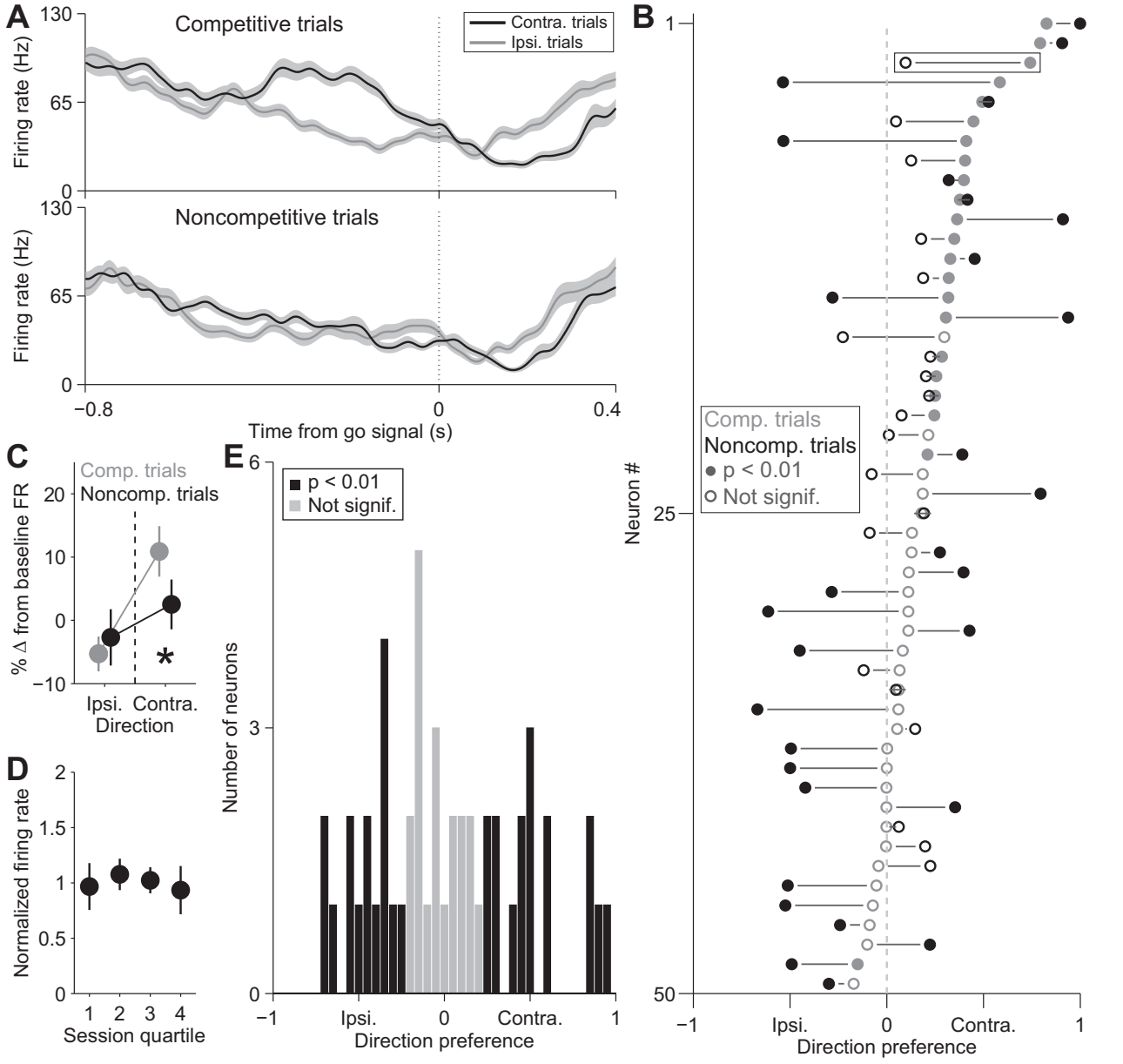

Fig. 4. Comparison of SC buildup neuron activity between competitive and noncompetitive trials.*A*: Peri-event histograms for an example buildup neuron grouped by trial type and movement direction. Shading, ± SEM. Histograms are smoothed with a Gaussian filter (σ = 15 ms). Ipsi., ipsiversive; Contra., contraversive.*B*: Direction preference during delay epoch for competitive vs. noncompetitive trials for SC buildup neurons. Each connected pair of circles shows one neuron. Neurons tend to exhibit contraversive preference in competitive, but not noncompetitive, trials. Boxed circle corresponds to example neuron in *A*.*C*: Change in firing rate between baseline and delay epoch grouped by trial type and movement direction. Baseline calculated as the average firing rate over the duration of the trial (from odor port entry to water port exit). Mean ± SEM across buildup neurons. *, $p < 0.05$, paired two-tailed t-test.*D*: Firing rates of buildup neurons across the duration of the session.*E*: Direction preference of buildup neurons calculated in noncompetitive trials while the mouse was in the odor port before receiving the odor.

performing fewer control than test sessions, these results are consistent with the contraversive preference we observed in SC recordings in competitive, but not noncompetitive, trials (Fig. 4*B*).

Finally, we wondered where the interactions among neuronal populations, which presumably mediate the competition among targets for movement, take place. In the context of a competition between leftward and rightward targets, one possibility is that the interactions occur between populations within the right and left SC, consistent with our findings and with previous empirical and theoretical work (Arai et al., 1994; Munoz and Istvan, 1998; Lo and Wang, 2006; Kim and Basso, 2008; Hirokawa et al., 2011; Marino et al., 2011; Felsen and Mainen, 2012; Kopec et al., 2015; Taouali et al., 2015; Fig. 6*A*). Indeed, neural circuitry in the SC is well-suited for mediating such interactions (Lee and Hall, 2006; Isa and Hall, 2009; Sooksawate et al., 2011; Bayguinov et al., 2015; Villalobos et al., 2018). Another possibility is that the interactions occur in any of the many structures that provide input to the SC (Edwards et al., 1979;

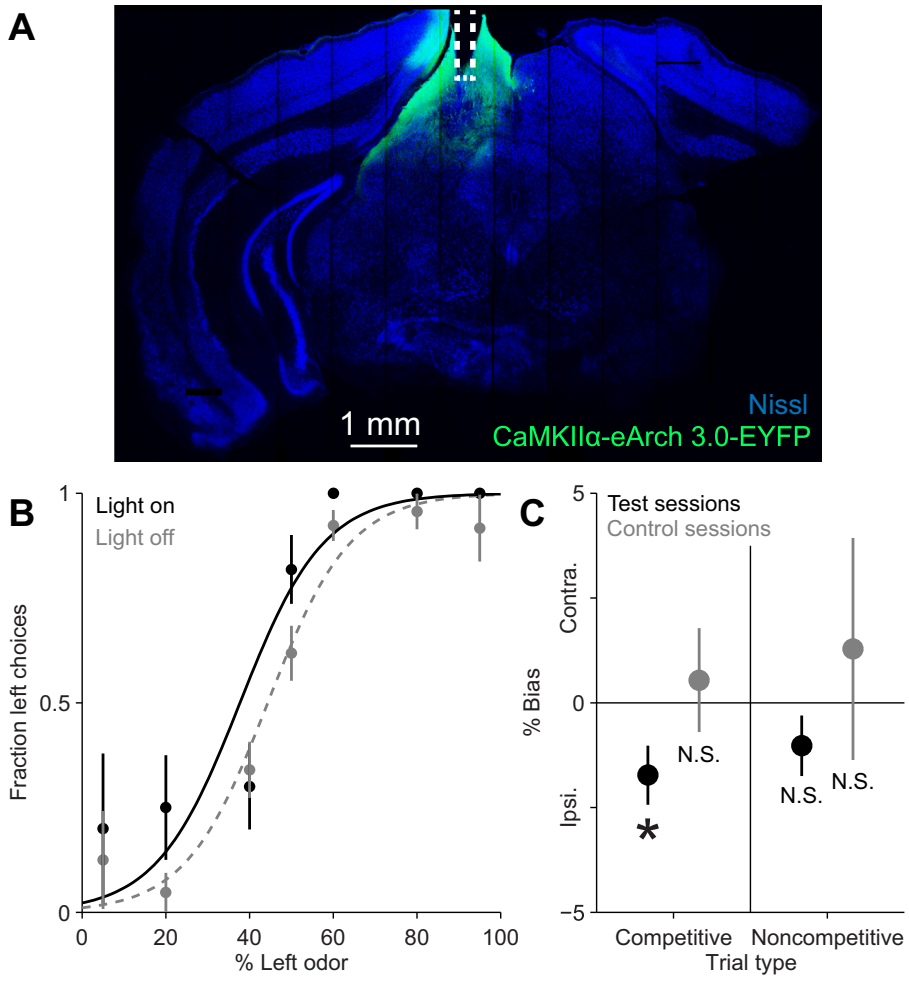

Fig. 5. Effect of Arch-mediated unilateral SC inhibition on behavior.*A*: Example confirmation of fiber implant and Arch expression. Coronal section (3.4 mm caudal from bregma) shows CaMKIIα-eArch3.0-EYFP expression (green) and fiber track in left SC. White line indicates fiber location.*B*: Behavioral performance in competitive trials with and without light delivery for example test session, as in Fig. 1*C*, showing that inhibiting left SC activity shifted choices leftward (ipsiversively).*C*: % directional bias due to inhibition, separately by trial type, for 77 test and 5 control sessions. Mean ± SEM across sessions. *, $p < 0.05$, paired two-tailed t-test comparing % bias to 0; N.S., not significant. Error bars are larger for control data due to fewer control sessions. (For interpretation of the references to color in this figure legend, the reader is referred to the web version of this article.)

Sparks and Hartwich-Young, 1989), including cortical regions (Fig. 6*A*, gray lines), with the outcome of the interactions inherited by the SC.

These possibilities – competition upstream of, and within, the SC – are not mutually exclusive: extrinsic input reflecting competition in afferent structures could subtly bias persistent interactions between the SCs that then serve to amplify this bias (Trappenberg et al., 2001; Lo and Wang, 2006; Fig. 6*A*). If movements made under non-competitive conditions do not engage the SC, then even when the same inter-SC interactions occur, they would not be extrinsically biased (Fig. 6*B*). We wondered whether such unbiased inter-SC interactions could explain our finding that SC neurons are about as likely to prefer ipsiversive as contraversive movement under noncompetitive conditions (Fig. 4*B*). The intuition is that "winner-take-all" inter-SC interactions would lead to some SC neurons exhibiting a direction preference, but without any bias in extrinsic inputs to either SC, that preference would as likely be ipsiversive as contraversive. We tested this intuition using an attractor model of SC activity (Wimmer et al., 2014; Experimental Procedures) in which the only difference between competitive and noncompetitive trials was that the input to the two SCs (e.g., from cortex) was imbalanced in the former (Fig. 6*A*) but balanced in the latter (Fig. 6*B*). We found that the modeled SC neurons exhibited, on average, a contraversive preference in competitive trials that was lost in noncompetitive trials, similar to the pattern exhibited by the buildup neurons we recorded (Fig. 6*C*). While these modeling results do not exclude other possible explanations for our data, they support the idea that biased competition between the two SCs can contribute to mediating spatial choice.

DISCUSSION

We recorded SC activity in freely-moving behaving mice, and observed qualitatively similar functional properties of SC neurons as have been described in other species. Specifically, when making spatial choices, we found that many neurons exhibit a burst of activity, and some a reduction in activity, at the time of movement initiation, and many exhibit an increase in activity as the contraversive choice is made and the movement is planned (Fig. 3). Consistent with these data, we found that unilaterally inhibiting the activity of excitatory SC neurons preceding movement initiation resulted in an ipsiversive choice bias during competitive trials, with the magnitude of the effect consistent with previous studies (Stubblefield et al., 2013; Kopec et al., 2015). These findings suggest that, although some SC functions, and the functional properties of some SC neurons, likely differ across species, the SC plays a broadly similar role in spatial choice in mice as in other species, and in full-body movements as in other forms of orienting movements (Sparks, 1999; Horwitz and Newsome, 2001; Carello and Krauzlis, 2004; Felsen and Mainen, 2012; Mysore and Knudsen, 2014; Philipp and Hoffmann, 2014; Duan et al., 2015; Kardamakis et al., 2015; Song and McPeek, 2015; Wolf et al., 2015; Duan et al., 2018).

However, we also found that the relationship between SC activity and movement direction is considerably different

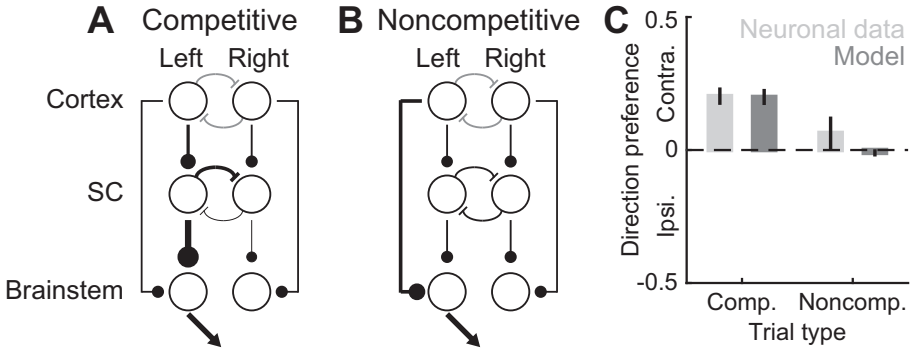

Fig. 6. Model showing proposed activity upstream of the SC (here, cortex), in the SC, and in the brainstem, and the resulting direction preference in SC neurons, under competitive and noncompetitive conditions.*A*: Proposed activity for rightward movement under competitive conditions. Input (here, from cortex) subtly biases the competition between the two SCs such that output from the left SC is much stronger than from the right SC. Line thickness represents level of activity. Filled circles, excitatory input; perpendicular lines, inhibitory input.*B*: Same as *A*, for noncompetitive conditions. Inter-SC competition continues but is unbiased because input to the two SCs is equal (movement-related information is instead conveyed directly to brainstem). On average, neither SC is more likely to produce a stronger output.*C*: Direction preferences of model SC neurons and recorded buildup neurons under competitive and noncompetitive conditions. Mean ± SEM across neurons. *, $p < 0.01$, two-tailed paired t-test.

when movements are made under noncompetitive conditions. Many buildup neurons no longer exhibit a preference for upcoming contraversive movements (Fig. 4*B*), and unilateral inhibition during noncompetitive trials did not cause a significant directional bias (Fig. 5*C*). These results support the idea that movements made under noncompetitive conditions may not require the SC (Duan et al., 2015), but could instead be mediated by direct projections from cortex to brainstem premotor circuits (Schiller et al., 1980; Hanes and Wurtz, 2001; Schiller and Tehovnik, 2005; Fig. 6). While SC activity is generally thought to promote contraversive movement (Gandhi and Katnani, 2011; Wang et al., 2015), several studies have shown that SC stimulation can also elicit ipsiversive movements (Sahibzada et al., 1986; Dean et al., 1989), perhaps related to the role of the SC in defensive and avoidance behavior (Cohen and Castro-Alamancos, 2010; DesJardin et al., 2013). By directly comparing the activity of the same neurons under competitive and noncompetitive conditions, our study demonstrates that the contraversive-promoting effect of SC activity may be competition-dependent. This conclusion is supported by the findings from our attractor model, which demonstrated that biased input to the two competing SCs resulted in an overall contraversive preference while unbiased input did not (Fig. 6), and is consistent with a large body of work suggesting that SC activity reflects the selection of a spatial target from among alternatives (Basso and Wurtz, 1997, 1998; Kim and Basso, 2008; Thevarajah et al., 2009; Nummela and Krauzlis, 2010; Kopec et al., 2015), an inherently competitive process.

In a previous study, we used the present behavioral task to examine activity in the substantia nigra pars reticulata (SNr), an output of the basal ganglia and one of the primary sources of inhibitory drive to the SC (Lintz and Felsen, 2016). Interestingly, we found that direction preference in the SNr was stronger on noncompetitive than competitive trials, suggesting that the activity we observed in the SC is not simply inherited from the SNr. If it were, then we would have observed stronger direction preference in noncompetitive than competitive trials in the SC as well, the opposite of what we found (Fig. 4*B*). These results support the idea that the basal ganglia may control movement via distinct downstream pathways differently depending on context (Redgrave et al., 2010). Specifically, under competitive conditions, the SNr may influence activity in the SC, while under noncompetitive conditions, the same basal ganglia output may influence extracollicular targets such as thalamocortical neurons that ultimately drive direct cortical projections to brainstem premotor circuits. The latter pathway is consistent with how habitual movements, akin to those required under noncompetitive trials in our task, are thought to be mediated (Yin and Knowlton, 2006). Notably, in noncompetitive trials the value assigned to each movement is likely to be strongly influenced by prior choices and outcomes, which are thought to affect how the basal ganglia modulate downstream motor activity (Hikosaka et al., 2006; Yttri and Dudman, 2018).

Our data support the appealing idea that competition among spatial targets specifically engages SC circuitry (Fig. 6). However, they do not rule out the possibility that the pattern of activity observed here is inherited from any of the regions, aside from the SNr, that provide input to the SC (Edwards et al., 1979; Sparks and Hartwich-Young, 1989; May, 2006; Savage et al., 2017). Indeed, the extent to which decision-related SC activity reflects the integration of computations performed upstream, as opposed to intrinsic interactions, is an open question (Wolf et al., 2015). Finally, while we have emphasized similarities between our results and previous findings in other species, whether and how SC anatomy and physiology differ between rodents and other species also remain open questions (Seabrook et al., 2017; Aguilar et al., 2018). Future studies can build on the present results by focusing on specific SC cell types and projections (Oliveira and Yonehara, 2018) in order to examine the mechanisms, both within and upstream of the SC, by which these context-dependent interactions are mediated.

ACKNOWLEDGMENTS

We thank members of the Felsen lab for constructive comments on the manuscript.

Funding: This work was supported by the National Institutes of Health (R01NS079518, F31NS103305), with technical support from the Optogenetics and Neural Engineering Core at the University of Colorado Anschutz Medical Campus, funded in part by the National Institutes of Health (P30NS048154).

Author contributions: ML conceived and designed the analysis, collected the data, analyzed the data, and wrote the manuscript. JE and JZ constructed the model, analyzed the modeling results, and edited the manuscript. GF conceived and designed the analysis, analyzed the data, and wrote the manuscript.

REFERENCES

Aguilar BL, Forcelli PA, Malkova L. (2018) Inhibition of the substantia nigra pars reticulata produces divergent effects on sensorimotor gating in rats and monkeys. Sci Rep 8(9369).

Al-Juboori SI, Dondzillo A, Stubblefield EA, Felsen G, Lei TC, Klug A. (2013) Light scattering properties vary across different regions of the adult mouse brain. PLoS One 8e67626.

Anikeeva P, Andalman AS, Witten I, Warden M, Goshen I, Grosenick L, Gunaydin LA, Frank LM, Deisseroth K. (2011) Optetrode: a multichannel readout for optogenetic control in freely moving mice. Nat Neurosci 15:163-170.

Arai K, Keller EL, Edelman JA. (1994) Two-dimensional neural network model of the primate saccadic system. Neural Netw 7:1115-1135.

Basso MA, May PJ. (2017) Circuits for action and cognition: a view from the superior colliculus. Annu Rev Vis Sci 3:197-226.

Basso MA, Wurtz RH. (1997) Modulation of neuronal activity by target uncertainty. Nature 389:66-69.

Basso MA, Wurtz RH. (1998) Modulation of neuronal activity in superior colliculus by changes in target probability. J Neurosci 18:7519-7534.

Bayguinov PO, Ghitani N, Jackson MB, Basso MA. (2015) A hard-wired priority map in the superior colliculus shaped by asymmetric inhibitory circuitry. J Neurophysiol 114:662-676.

Carello CD, Krauzlis RJ. (2004) Manipulating intent: evidence for a causal role of the superior colliculus in target selection. Neuron 43:575-583.

Cohen JD, Castro-Alamancos MA. (2010) Neural correlates of active avoidance behavior in superior colliculus. J Neurosci 30:8502-8511.

Dean P, Redgrave P, Westby GW. (1989) Event or emergency? Two response systems in the mammalian superior colliculus. Trends Neurosci 12:137-147.

DesJardin JT, Holmes AL, Forcelli PA, Cole CE, Gale JT, Wellman LL, Gale K, Malkova L. (2013) Defense-like behaviors evoked by pharmacological disinhibition of the superior colliculus in the primate. J Neurosci 33:150-155.

Dorris MC, Munoz DP. (1998) Saccadic probability influences motor preparation signals and time to saccadic initiation. J Neurosci 18:7015-7026.

Dorris MC, Pare M, Munoz DP. (1997) Neuronal activity in monkey superior colliculus related to the initiation of saccadic eye movements. J Neurosci 17:8566-8579.

Duan CA, Erlich JC, Brody CD. (2015) Requirement of prefrontal and midbrain regions for rapid executive control of behavior in the rat. Neuron 86:1491-1503.

Duan CA, Pagan M, Piet AT, Kopec CD, Akrami A, Riordan AJ, Erlich JC, Brody CD. (2018) Collicular circuits for flexible sensorimotor routing. bioRxiv 245613.

Edwards SB, Ginsburgh CL, Henkel CK, Stein BE. (1979) Sources of subcortical projections to the superior colliculus in the cat. J Comp Neurol 184:309-329.

Feierstein CE, Quirk MC, Uchida N, Sosulski DL, Mainen ZF. (2006) Representation of spatial goals in rat orbitofrontal cortex. Neuron 51:495-507.

Felsen G, Mainen ZF. (2008) Neural substrates of sensory-guided locomotor decisions in the rat superior colliculus. Neuron 60:137-148.

Felsen G, Mainen ZF. (2012) Midbrain contributions to sensorimotor decision making. J *Neurophysiol* 108:135-147.

Gandhi NJ, Katnani HA. (2011) Motor functions of the superior colliculus. Annu Rev Neurosci 34:205-231.

Glimcher PW, Sparks DL. (1992) Movement selection in advance of action in the superior colliculus. Nature 355:542-545.

Grantyn AA, Dalezios Y, Kitama T, Moschovakis AK. (1996) Neuronal mechanisms of two-dimensional orienting movements in the cat. I. A quantitative study of saccades and slow drifts produced in response to the electrical stimulation of the superior colliculus. Brain Res Bull 41:65-82.

Green DM, Swets JA. (1966) Signal detection theory and psychophysics. New York, NY: Wiley, 1966.

Hafed ZM, Krauzlis RJ. (2012) Similarity of superior colliculus involvement in microsaccade and saccade generation. J Neurophysiol 107:1904-1916.

Hafed ZM, Goffart L, Krauzlis RJ. (2009) A neural mechanism for microsaccade generation in the primate superior colliculus. Science 323:940-943.

Hanes DP, Wurtz RH. (2001) Interaction of the frontal eye field and superior colliculus for saccade generation. J Neurophysiol 85:804-815.

Hikosaka O, Nakamura K, Nakahara H. (2006) Basal ganglia orient eyes to reward. J Neurophysiol 95:567-584.

Hirokawa J, Sadakane O, Sakata S, Bosch M, Sakurai Y, Yamamori T. (2011) Multisensory information facilitates reaction speed by enlarging activity difference between superior colliculus hemispheres in rats. PLoS One 6e25283.

Horwitz GD, Newsome WT. (1999) Separate signals for target selection and movement specification in the superior colliculus. Science 284:1158-1161.

Horwitz GD, Newsome WT. (2001) Target selection for saccadic eye movements: prelude activity in the superior colliculus during a direction–discrimination task. J Neurophysiol 86:2543-2558.

Ikeda T, Hikosaka O. (2003) Reward-dependent gain and bias of visual responses in primate superior colliculus. Neuron 39:693-700.

Isa T, Hall WC. (2009) Exploring the superior colliculus in vitro. J Neurophysiol 102:2581-2593.

Ito M, Doya K. (2015) Distinct neural representation in the dorsolateral, dorsomedial, and ventral parts of the striatum during fixed- and free-choice tasks. J Neurosci 35:3499-3514.

Kardamakis AA, Saitoh K, Grillner S. (2015) Tectal microcircuit generating visual selection commands on gaze-controlling neurons. Proc Natl Acad Sci U S A 112:E1956-E1965.

Kim B, Basso MA. (2008) Saccade target selection in the superior colliculus: a signal detection theory approach. J Neurosci 28:2991-3007.

Kopec CD, Erlich JC, Brunton BW, Deisseroth K, Brody CD. (2015) Cortical and subcortical contributions to short-term memory for orienting movements. Neuron 88:367-377.

Krauzlis RJ, Liston D, Carello CD. (2004) Target selection and the superior colliculus: goals, choices and hypotheses. Vision Res 44:1445-1451.

Krauzlis RJ, Lovejoy LP, Zénon A. (2013) Superior colliculus and visual spatial attention. Annu Rev Neurosci 36:165-182.

Lee P, Hall WC. (2006) An in vitro study of horizontal connections in the intermediate layer of the superior colliculus. J Neurosci 26:4763-4768.

Lee C, Rohrer WH, Sparks DL. (1988) Population coding of saccadic eye movements by neurons in the superior colliculus. Nature 332:357-360.

Lintz MJ, Felsen G. (2016) Basal ganglia output reflects internally-specified movements. eLife 5e13833.

Lo CC, Wang XJ. (2006) Cortico-basal ganglia circuit mechanism for a decision threshold in reaction time tasks. Nat Neurosci 9:956-963.

Marino RA, Trappenberg TP, Dorris M, Munoz DP. (2011) Spatial interactions in the superior colliculus predict saccade behavior in a neural field model. J Cog Neurosci 24:315-336.

May PJ. (2006) The mammalian superior colliculus: laminar structure and connections. Prog Brain Res 151:321-378.

McHaffie JG, Stein BE. (1982) Eye movements evoked by electrical stimulation in the superior colliculus of rats and hamsters. Brain Res 247:243-253.

McPeek RM, Keller EL. (2002) Saccade target selection in the superior colliculus during a visual search task. J Neurophysiol 88:2019-2034.

McPeek RM, Keller EL. (2004) Deficits in saccade target selection after inactivation of superior colliculus. Nat Neurosci 7:757-763.

Mize RR. (1992) The organization of GABAergic neurons in the mammalian superior colliculus. Prog Brain Res 90:219-248.

Munoz DP, Guitton D. (1991) Control of orienting gaze shifts by the tectoreticulospinal system in the head-free cat. II. Sustained discharges during motor preparation and fixation. J Neurophysiol 66:1624-1641.
Munoz DP, Istvan PJ. (1998) Lateral inhibitory interactions in the intermediate layers of the monkey superior colliculus. J Neurophysiol 79:1193-1209.
Munoz DP, Wurtz RH. (1993) Fixation cells in monkey superior colliculus. I. Characteristics of cell discharge. J Neurophysiol 70:559-575.
Munoz DP, Wurtz RH. (1995) Saccade-related activity in monkey superior colliculus. I. Characteristics of burst and buildup cells. J Neurophysiol 73:2313-2333.
Munoz DP, Guitton D, Pelisson D. (1991) Control of orienting gaze shifts by the tectoreticulospinal system in the head-free cat. III. Spatiotemporal characteristics of phasic motor discharges. J Neurophysiol 66:1642-1666.
Mysore SP, Knudsen EI. (2011) The role of a midbrain network in competitive stimulus selection. Curr Opin Neurobiol 21:653-660.
Mysore SP, Knudsen EI. (2014) Descending control of neural bias and selectivity in a spatial attention network: rules and mechanisms. Neuron 84:214-226.
Nummela SU, Krauzlis RJ. (2010) Inactivation of primate superior colliculus biases target choice for smooth pursuit, saccades, and button press responses. J Neurophysiol 104:1538-1548.
Odegaard B, Grimaldi P, Cho SH, Peters MAK, Lau H, Basso MA. (2018) Superior colliculus neuronal ensemble activity signals optimal rather than subjective confidence. Proc Natl Acad Sci U S A 115:E1588-E1597.
Oliveira AF, Yonehara K. (2018) The mouse superior colliculus as a model system for investigating cell type-based mechanisms of visual motor transformation. Front Neural Circuits 12(59).
Pastor-Bernier A, Cisek P. (2011) Neural correlates of biased competition in premotor cortex. J Neurosci 31:7083-7088.
Paxinos G, Franklin KBJ. (2004) The mouse brain in stereotaxic coordinates. San Diego, CA: Academic Press, 2004.
Philipp R, Hoffmann K-P. (2014) Arm movements induced by electrical microstimulation in the superior colliculus of the macaque monkey. J Neurosci 34:3350-3363.
Redgrave P, Rodriguez M, Smith Y, Rodriguez-Oroz MC, Lehericy S, Bergman H, Agid Y, DeLong MR, Obeso JA. (2010) Goal-directed and habitual control in the basal ganglia: implications for Parkinson's disease. Nat Rev Neurosci 11:760-772.
Robinson DA. (1972) Eye movements evoked by collicular stimulation in the alert monkey. Vision Res 12:1795-1808.
Sahibzada N, Dean P, Redgrave P. (1986) Movements resembling orientation or avoidance elicited by electrical stimulation of the superior colliculus in rats. J Neurosci 6:723-733.
Savage MA, McQuade R, Thiele A. (2017) Segregated fronto-cortical and midbrain connections in the mouse and their relation to approach and avoidance orienting behaviors. J Comp Neurol 525:1980-1999.
Schiller PH, Tehovnik EJ. (2005) Neural mechanisms underlying target selection with saccadic eye movements. Prog Brain Res 149:157-171.
Schiller PH, True SD, Conway JL. (1980) Deficits in eye movements following frontal eye-field and superior colliculus ablations. J Neurophysiol 44:1175-1189.
Schmitzer-Torbert N, Jackson J, Henze D, Harris K, Redish AD. (2005) Quantitative measures of cluster quality for use in extracellular recordings. Neuroscience 131:1-11.
Seabrook TA, Burbridge TJ, Crair MC, Huberman AD. (2017) Architecture, function, and assembly of the mouse visual system. Annu Rev Neurosci 40:499-538.
Siniscalchi MJ, Phoumthipphavong V, Ali F, Lozano M, Kwan AC. (2016) Fast and slow transitions in frontal ensemble activity during flexible sensorimotor behavior. Nat Neurosci 19:1234-1242.
Song J-H, McPeek RM. (2015) Neural correlates of target selection for reaching movements in superior colliculus. J Neurophysiol 113:1414-1422.
Sooksawate T, Isa K, Behan M, Yanagawa Y, Isa T. (2011) Organization of GABAergic inhibition in the motor output layer of the superior colliculus. Eur J Neurosci 33:421-432.
Sparks DL. (1986) Translation of sensory signals into commands for control of saccadic eye movements: role of primate superior colliculus. Physiol Rev 66:118-171.
Sparks DL. (1999) Conceptual issues related to the role of the superior colliculus in the control of gaze. Curr Opin Neurobiol 9:698-707.
Sparks DL, Hartwich-Young R. (1989) The deep layers of the superior colliculus. Rev Oculomot Res 3:213-255.
Straschill M, Rieger P. (1973) Eye movements evoked by focal stimulation of the cat's superior colliculus. Brain Res 59:211-227.
Stubblefield EA, Costabile JD, Felsen G. (2013) Optogenetic investigation of the role of the superior colliculus in orienting movements. Behav Brain Res 255:55-63.
Stubblefield EA, Thompson JA, Felsen G. (2015) Optogenetic cholinergic modulation of the mouse superior colliculus in vivo. J Neurophysiol 114:978-988.
Taouali W, Goffart L, Alexandre F, Rougier NP. (2015) A parsimonious computational model of visual target position encoding in the superior colliculus. Biol Cybern 109:549-559.
Thevarajah D, Mikulic A, Dorris MC. (2009) Role of the superior colliculus in choosing mixed-strategy saccades. J Neurosci 29:1998-2008.
Thompson JA, Felsen G. (2013) Activity in mouse pedunculopontine tegmental nucleus reflects action and outcome in a decision-making task. J Neurophysiol 110:2817-2829.
Thompson JA, Costabile JD, Felsen G. (2016) Mesencephalic representations of recent experience influence decision making. eLife 5: e16572.
Trappenberg TP, Dorris MC, Munoz DP, Klein RM. (2001) A model of saccade initiation based on the competitive integration of exogenous and endogenous signals in the superior colliculus. J Cog Neurosci 13:256-271.
Uchida N, Mainen ZF. (2003) Speed and accuracy of olfactory discrimination in the rat. Nat Neurosci 6:1224-1229.
Villalobos CA, Wu Q, Lee PH, May PJ, Basso MA. (2018) Parvalbumin and GABA microcircuits in the mouse superior colliculus. Front Neural Circuits 12(35).
Wang L, Liu M, Segraves MA, Cang J. (2015) Visual experience is required for the development of eye movement maps in the mouse superior colliculus. J Neurosci 35:12281-12286.
Wimmer K, Nykamp DQ, Constantinidis C, Compte A. (2014) Bump attractor dynamics in prefrontal cortex explains behavioral precision in spatial working memory. Nat Neurosci 17:431.
Wolf AB, Lintz MJ, Costabile JD, Thompson JA, Stubblefield EA, Felsen G. (2015) An integrative role for the superior colliculus in selecting targets for movements. J Neurophysiol 114:2118-2131.
Wurtz RH, Goldberg ME. (1971) Superior colliculus cell responses related to eye movements in awake monkeys. Science 171:82-84.
Yin HH, Knowlton BJ. (2006) The role of the basal ganglia in habit formation. Nat Rev Neurosci 7:464-476.
Yttri EA, Dudman JT. (2018) A proposed circuit computation in basal ganglia: history-dependent gain. Mov Disord 33:704-716.

(Received 30 October 2018, Accepted 1 April 2019)
(Available online 11 April 2019)